JOURNAL OF APPLIED PHYSICS **109**, 124906 (2011)

Time-resolved x-ray excited optical luminescence in InGaN/GaN multiple quantum well structures

S. M. O'Malley,[1,a)] P. Revesz,[3] A. Kazimirov,[3] and A. A. Sirenko[4]
[1]*Department of Physics, Rutgers – The State University of New Jersey, Camden, New Jersey 08102, USA*
[2]*Cornell High Energy Synchrotron Source (CHESS), Cornell University, Ithaca, New York 14853, USA*
[3]*Department of Physics, New Jersey Institute of Technology, Newark, New Jersey 07102, USA*

(Received 6 January 2011; accepted 11 May 2011; published online 21 June 2011)

Synchrotron-based x-ray radiation has been utilized to measure time-resolved x-ray excited optical luminescence (TR-XEOL) from InGaN/GaN multiple quantum well (MQW) structures. Excess carrier recombination lifetimes were determined for MQWs grown on conventional *c*-plane as well as on non-polar *m*-plane substrates. In addition, the simultaneous measurement of XEOL and x-ray fluorescence reveals an interaction between inner-core excitations of Si impurities and bound exciton recombination in doped GaN-based device structures. Furthermore, the TR-XEOL characterization technique were also applied to InGaN/GaN MQWs grown on GaN inverted pyramid structures. © *2011 American Institute of Physics*. [doi:10.1063/1.3598137]

I. INTRODUCTION

X-ray excited optical luminescence (XEOL) in semiconductors is similar to its laser-based counterpart photoluminescence (PL): the external radiation excites nonequilibrium carriers that recombine and emit photons with energy close to the bandgap. In traditional PL, the laser photon energy is usually chosen to be slightly above the bandgap of the semiconductor under investigation. This approach restricts carrier excitation and relaxation to the valence and conduction bands. In the case of XEOL, the incident photon energy can be $\sim 10^3$ to 10^4 times greater than the bandgap energy of the material; excitations in this case follow a different relaxation path which may lead to photoexcited carriers that recombine within the bandgap. Additionally, the penetration depth for hard x-ray radiation is significantly greater than those for optical photon energies traditionally used in laser-based luminescence techniques. This allows XEOL measurements to be carried-out on fully- or near fully-completed device structures which contain thick cladding layers, heavily doped contact layers, and even metalized contacts.[1,2]

Hard x-rays incident upon a material are capable of knocking out an electron from the inner core of an atom. This leaves behind a core level vacancy that must be filled by another electron making a transition down from a higher energy state. During the relaxation process, the energy difference between the initial and final electronic states can be dissipated through the emission of x-rays with energy equal to the difference. This radiation is known as *x-ray fluorescence* and its discrete energy values are referred to as *characteristic lines* because their wavelengths are related to the unique atomic number (Z) of the excited atom.

The initial relaxation process, leading to x-ray fluorescence, leaves a similar vacancy in a higher energy shell that gives up its electron to the inner shell. This additional vacancy must again be filled by a higher energy electron. In this sense, relaxation proceeds in a cascading manner with the subsequent occurrence of less energetic radiative and/or non-radiative decay processes. As this event progresses, the outermost electrons from the excited atom become involved and energy transfer out of the atom and into the lattice may take place. Hence, the initial x-ray excitation can follow a relaxation pathway out of the excited atom and generate visible luminescence in the parent material.[3–5] This process is in stark contrast to that found in photoluminescence which only involves the outer-most electrons shared between neighboring atoms within the lattice. X-ray excited optical luminescence has been utilized in various applications such as in x-ray scintillation detectors; however, the technique has not been widely used for materials characterization. A few exceptions are recent activities at APS-Argonne National Lab[5,6] and SPring-8, Japan.[7]

In the case of XEOL, synchrotron-based x-ray sources hold a number of advantages e.g., the incident photon energies at synchrotron facilities can be tuned over a wide range from a few keV to 100 keV. Thereby, as in the case of x-ray absorption fine structure spectroscopy (XAFS), one can selectively excite core level transitions from different elements within the crystalline lattice and gain sensitivity to chemical variations within a semiconductor device structure. In 2008, Lankinen *et al*. related the appearance of an additional luminescence peak at 3.35 eV, in their XEOL spectra, with the electrical activation of Mg-dopant in GaN upon thermal annealing. This emission peak was not observed using traditional laser-based PL techniques.[1] In addition, the high intensity of synchrotron radiation coupled with recent advances in x-ray focusing optics has enabled incident beams to be focused down to submicron sizes while still retaining reasonable flux densities and therefore, good signal-noise ratios suitable for spatial mapping of device structures.[8] Lastly, the radiation from synchrotron sources is pulsed in nature, with nominal pulse duration in range of tens of picoseconds; thereby enabling detection of time-resolved x-ray excited optical luminescence (TR-XEOL). For example, in 2006, Rosenberg *et al*. demonstrated

a)Electronic mail: omallese@camden.rutgers.edu.

 © 2011 American Institute of Physics

Downloaded 09 Sep 2011 to 130.199.3.165. Redistribution subject to AIP license or copyright; see http://jap.aip.org/about/rights_and_permissions

how TR-XEOL could be used to determine the luminescence origin of complex heterostructures and recombination pathways in a coaxial-type Si-CdSe nanowire structure.[5] The goal of this work is twofold: (1) demonstrate that synchrotron-based XEOL is a viable characterization tool to study radiative recombination in GaN-based device structures and (2) assert that XEOL, if combined with fluorescence data, can provide new insight into the role played by impurities in optical luminescence.

II. SAMPLE DESCRIPTION

Two separate planar InGaN/GaN multiple quantum well (MQW) structures were grown by MOVPE on freestanding GaN substrates. One sample was grown on *c*-planar GaN while another identical MQW structure was grown on an *m*-planar GaN substrate. The MQW structures contain five InGaN wells (5 nm) separated by GaN barriers (15 nm). The target Indium composition for the QWs was ~20% for both the *c*- and *m*-planar growth. The structure was finished with an Mg-doped GaN capping layer. An additional sample was also studied; it consisted of an InGaN/GaN MQW structure grown on an inverted-pyramid shaped GaN template layer (see Ref. 9 for further details about similar inverted-pyramid shaped structures). The base width of the pyramids is ~6.2 μm and the sidewalls contain $\{1\ -1\ 0\ 1\}$ facets. The sidewall MQW structure contains five InGaN wells (~4 nm) with GaN barriers (~7 nm). Terminating the sidewall grown MQW structure is a ~15 nm thick AlGaN blocking layer and a ~200 nm thick *p*-doped GaN capping layer. These inverted-structures show promise in broad-band applications due to variation of both the QW indium composition and thickness along their sidewall facets.[9] Note the structure is similar to that of inverted "V-shaped" pits formed around threading dislocations.

III. EXPERIMENTAL SETUP

Electrons within a synchrotron are spaced around the storage ring in *bunches*; several groups of these bunches form a *train*. Typically synchrotrons will contain several of these electron trains revolving around the storage ring and produce radiation. Our time-resolved x-ray excited optical luminescence (TR-XEOL) measurements were carried out at the A2 beamline at Cornell high energy synchrotron source (CHESS). During our beam time at CHESS each train was comprised of five bunches except the last train which contained six bunches. Each bunch produces an x-ray pulse of 65 ps in duration. The spacing between bunches within a train was 14 ns; hence, a single train of five bunches has a width of ~56 ns. The orbital period of the electrons around the storage ring is 2.56 μs; however, the injection pattern has a gap of ~1.1 μs between the last bunch in the last train and the return of the first bunch in the first train. Such a pattern enabled time-resolved measurements in both, the sub-ns and μs ranges of the carrier lifetimes.

The A2 beamline is equipped to perform x-ray diffraction measurements; to this we integrated an optical luminescence detection setup based on a Bruker Czerny-Tuner type spectrograph and a streak camera (Hamamatsu's model C10627 streakscope). The camera was operated at a sweep rate matching the orbital frequency ($f = 391$ kHz) of the electronics around the electron storage ring. The samples were mounted within a Huber 4-circle diffractometer to which was mounted a collimating lens onto the chi-circle in order to collect sample luminescence. In this configuration the collection lens remains normal to the sample surface as the incident angle theta (θ) is scanned. The collection lens was coupled to a UV-VIS fiber optic cable, where the fiber output was focused onto the entrance slits of the spectrograph. A low-spectral resolution grating (50 groves/mm) was utilized for all time-resolved measurements in order to maximize the optical throughput. All measurements were performed at room temperature.

IV. EXPERIMENTAL RESULTS

Typical XEOL spectrum from the planar samples are shown in Fig. 1. The profile is dominated by two major features: (1) a sharp peak centered at 365 nm, which is related to GaN bandgap luminescence and (2) a broad peak at ~560 nm that originates from the InGaN/GaN MQW region. Time-resolved measurements were taken by centering the spectrograph wavelength to either the GaN (365 nm) or the InGaN MQW (560 nm) regions and then integrating the signal around these peak positions in order to obtain the transient dependence of the luminescence. Figure 2, depicts luminescence decay for both *c*- and *m*-planar grown samples, at an incident x-ray energy of 10.77 keV (hence, above the Ga $K\alpha$ absorption edge). The excess carrier recombination lifetime τ from the GaN region for the *c*-planar growth structure [Fig. 2(a)] is $\tau = 5.2$ ns, while the *m*-grown sample [Fig. 2(b)] displays a much shorter $\tau = 1.0$ ns lifetime. Note the presence of a second decay peak in Fig. 2(a). This peak is due to the arrival of the next electron bunch in the pulse train and it was left in Fig. 2(a) for illustrative purposes.

Luminescence decay measured from the InGaN/GaN MQW region is several orders of magnitude longer than that from the GaN spectral region. The typical lifetime for the InGaN/GaN active region greatly exceeds the 14 ns spacing between individual synchrotron bunches. The corresponding

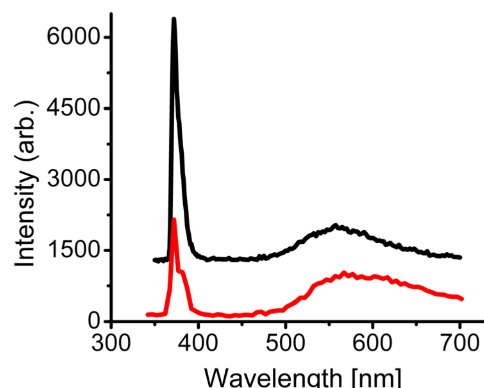

FIG. 1. (Color online) XEOL spectra for both *c*-planar (top/black curve) and *m*-planar (bottom/red curve) grown GaN/InGaN structures. The strong peaks at 365 nm originate from the GaN substrate; while the broad peaks at ~560 nm originate from the InGaN/GaN MQW structures. Spectra were offset for clarity. These measurements were carried out at the Advanced Photon Source (APS) at Argonne National Laboratory.

Downloaded 09 Sep 2011 to 130.199.3.165. Redistribution subject to AIP license or copyright; see http://jap.aip.org/about/rights_and_permissions

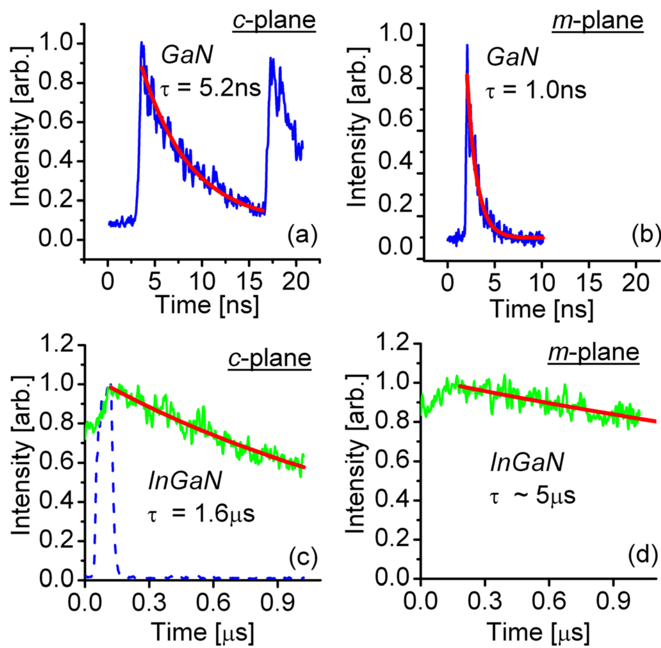

FIG. 2. (a) (Color online) Time-resolved XEOL decay at 365 nm (GaN) from the c-planar grown sample. The second peak depicts the next x-ray bunch pulse within the train. (b) TR-XEOL decay at 365 nm (GaN) from the m-planar grown sample. (c) TR-XEOL decay at 560 nm (InGaN/GaN MQW) from the c-planar grown sample. The dashed (blue) line is the GaN signal shown to illustrate the x-ray excitation pulse. (d) Luminescence decay at 560 nm (InGaN/GaN MQW) from the m-planar sample. Note: solid (red) line depicts fit to a single-exponential function. All measurement carried out at an x-ray energy of 10.77 keV.

analysis requires that an entire train be considered as the "excitation pulse" with the combined duration of $\sim$70 ns, which is still much shorter than the typical lifetime from InGaN/GaN active region. By synchronizing the streak camera with the last pulse train a window of 1.1 μs is available for the luminescence signal to decay. Though there is some overlap in the signal from previous pulse trains this does not affect the lifetime measurement. The MQW carrier lifetime, for the c-planar sample, is 1.6 μs [Fig. 3(c)]. The MQW structure grown on the m-plane GaN substrate has a carrier recombination lifetime of $\sim$5 μs.

In addition to carrier recombination lifetimes, the optical luminescence yield was measured as a function of x-ray energy in the vicinity of the $K\alpha$ absorption edge of Ga (10.378 keV). X-ray fluorescence was simultaneously monitored to determine absorption edge location while collecting the XEOL signal. The luminescence yield from the MQW region follows the profile of the x-ray fluorescence yield with a positive step at the $K\alpha$ transition [see Figs. 3(a) and 3(b)]. Luminescence yield from the GaN spectral region only displays a slight variation across the edge [Fig. 3(c)]. The m-plane grown sample, produced a similar GaN yield result across the edge; however, the luminescence yield from the active region displayed a negative step with a $\sim$31% decrease in yield across the edge (results not shown).

Recombination lifetimes were also measured for the inverted-pyramid sample. The XEOL spectra contained three peaks: a strong broad peak centered at $\sim$560 nm, a weaker feature at 450 nm and another peak at 365 nm originating

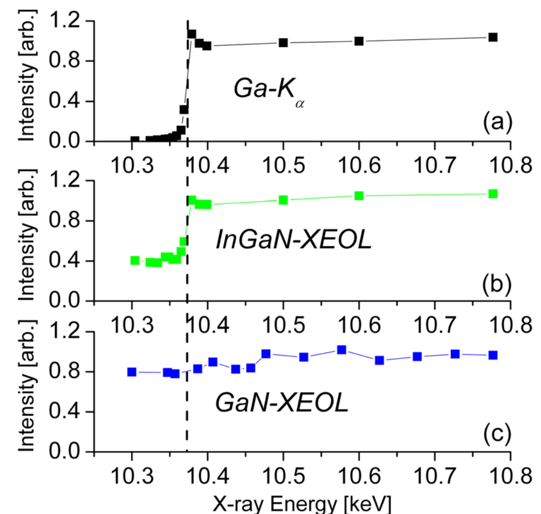

FIG. 3. (a) (Color online) Ga-Kα fluorescence yield, (b) InGaN MQW x-ray excited optical luminescence (XEOL) yield, (c) GaN XEOL yield. All measured from the c-planar grown InGaN/GaN MQW sample.

from the GaN layers. The peak at 560 nm has been assigned to MQW growth on the top (c-plane) facet of the inverted-pyramid structure. The 450 nm peak is believed to originating from MQW growth on the sidewall facets. The GaN signal had a lifetime of $\sim$1.6 ns and was fitted using a single exponential function. The 450 nm feature fits well with a single exponential decay with the lifetime of $\sim$1.4 ns [see Fig. 4(a)]. This lifetime is comparable to that found by low-temperature PL in InGaN/GaN MQWs grown on a triangular ridge structure with identical $\{1\ -1\ 0\ 1\}$ sidewall facets (see Ref. 10 for details). Luminescence decay from the c-planar grown InGaN QWs [Fig. 4(b)] requires a bi-exponential fit containing short ($\tau_{Short} \sim 30$ ns) and long ($\tau_{Long} \sim 5.6$ μs) components to adequately fit its temporal profile. The luminescence yield in both the GaN and MQW spectral regions

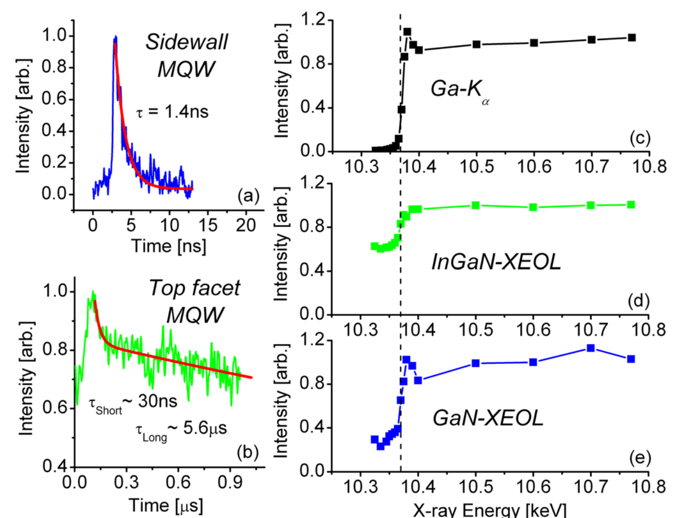

FIG. 4. (Color online) XEOL results for the inverted-pyramid sample. (a) Luminescence decay originating from the sidewall facet grown InGaN MQW structure (spectral region: 450 nm). (b) Luminescence decay from the c-planar grown InGaN/GaN MQW region (560 nm). Both TR-XEOL measurements performed at 10.77 keV (c) Ga-Kα fluorescence yield. (d) c-planar InGaN XEOL yield. (e) GaN optical luminescence yield.

Downloaded 09 Sep 2011 to 130.199.3.165. Redistribution subject to AIP license or copyright; see http://jap.aip.org/about/rights_and_permissions

shows a substantial yield increase at the Ga $K\alpha$ absorption edge [see Figs. 4(c)–(e)].

V. DISCUSSION

It is well known that group-III nitrides contain large piezoelectric (PE) fields along the (0 0 0 1) *c*-direction. When an optically active region, such as a multiple quantum well structure, is grown on the *c*-plane, the optical efficiency of the structure typically suffers. Hence, there has been a trend toward the growth of active layers on semi-polar or non-polar planes (e.g., the *m*-plane). In the case of carrier recombination, the presence of a strong PE field increases the lifetime as a result of coulombic forces increasing spatial separation and reducing the wavefunction overlap of the electrons and holes. Comparing the MQW carrier lifetimes between the *c*- and *m*-planar grown samples [see Figs. 2(c) and 2(d)], the *m*-planar sample exhibits a longer lifetime. The *m*-plane is non-polar; hence one expects its lifetime to be shorter in comparison to an identically grown structure on the *c*-plane. This result suggests that PE fields are not the dominant mechanism at work in the long carrier lifetime found in our *m*-planar sample. Most likely the longer lifetime is due to a greater number of defects in the *m*-planar substrate which propagate into the active region of the MQW structure.

The bi-exponential luminescence decay from the top facet (*c*-plane) grown InGaN MQW structure in the inverted-pyramid sample [see Fig. 4(b)] is a feature that is typically explained in planar samples as a short lived screening effect of the intrinsic PE field due to high carrier densities generated by large excitation densities.[11,12] The semi-polar nature of the sidewall facets $\{1\ -1\ 0\ 1\}$, that form the inverted pyramid structure, does not lead to such screening effects; hence luminescence from this region displays a single exponential decay component as expected [see Fig. 4(a)].

When the incident x-ray energy is scanned across an absorption edge, Ga-$K\alpha$ fluorescence displays a jump at the edge energy as shown in Figs. 3(a) and 4(c). Similar behavior is also expected for the XEOL signal. For a given x-ray energy, the total optical luminescence yield is a sum of contributions originating from various core-level excitations (e.g., K and/or L absorption of Ga) within the lattice. A change in yield at a given absorption edge may then be associated with that particular excitation. The observed XEOL yield dependencies, which are shown in Fig. 3(b) and Figs. 4(e) and 4(d), fit well into this interpretation. The trend at 365 nm [shown in Fig. 3(c)] for the *c*-planar MQW structure at first glance is however unexpected because the GaN-bandgap luminescence varies little across the absorption edge. Additionally, the *m*-planar sample revealed a similar trend at 365 nm with no well-defined threshold feature at the Ga $K\alpha$ absorption edge. Taking into account that these device structures include both *n*- and *p*-doped GaN layers, the bottom layer is *n*-type (Si-doped) while the capping layer is *p*-type (Mg-doped) GaN, it can then be concluded that the dominant XEOL contribution to the observed OL peak at $\sim$365 nm is from excitons bound to shallow impurities within the doped GaN layers. In view of the relative strength of the GaN luminescence peak it can be suggested that the leading role is played by excitons bound to donor impurities in the *n*-doped GaN substrate. These bound excitons are excited directly through Kα-absorption of the Si atoms (1.850 keV).

We have checked this assumption by measuring XEOL in several undoped GaN layers. All of them contained the same natural step-like XEOL profile similar to that in Fig. 4(e). Therefore, it can be suggested that the dominant XEOL mechanism at work in *n*-doped GaN, is the excitation of silicon impurities that results in the efficient creation and recombination of the bound excitons. This channel dominates by at least a factor of ten over the alternative mechanism of a free exciton creation and consequent recombination as we observed in undoped GaN. One may incorrectly conclude that the positive XEOL edge-jump from the InGaN region of the *c*-planar sample [Fig. 3(b)] and the lack of a jump for the GaN luminescence signal [Fig. 3(c)] may be due to the re-absorption of the higher energy GaN emission by the InGaN MQW layers. This is not the case however given our previous explanation relating the lack of a positive jump at the Ga-Kα edge for *n*-doped GaN to the presence of donor-bound excitons mediated by Si-Kα absorption. Instead, the optical luminescence from the InGaN layers simply originates from carrier generation by core-level excitations of Ga ions and the subsequent recombination of localized excitons. The negative edge jump observed in the *m*-plane MQW structure is likely related to the larger number of defects present in structures grown along this direction which has led to an increase in nonradiative recombination.

VI. CONCLUSION

In conclusion, XEOL can be a powerful characterization technique in the study of the bandgap luminescence in GaN-based device structures. Carrier dynamics measurements performed utilizing TR-XEOL can be a viable option as long as the spacing between x-ray pulses is comparable to the carrier recombination lifetime under investigation. Our combined XEOL and x-ray fluorescence measurements illustrate that dopant impurities play an important role in the radiative recombination of excess carriers by forming bound excitons initiated through inner-core excitation of Si impurities. In future studies, we will utilize micro-beam x-rays to simultaneously collect HRXRD and TR-XEOL measurements from multiple locations along the pyramid sidewall. Such measurements will allow for spatial mapping of local variations in the quantum well width and fluctuations of the indium composition in InGaN layers.

ACKNOWLEDGMENTS

The authors would also like to acknowledge both Thomas Wunderer and Ferdinand Scholz from the Institute of Optoelectronics, University of Ulm, for useful discussion and for supplying the inverted-pyramid sample. Additionally, we would like to thank Zhonghou Cai from the advanced photon source (APS) at Argonne National Laboratory for help with preliminary XEOL measurements.

[1] A. Lankinen, O. Svensk, M. Mattila, T. O. Tuomi, H. Lipsanen, P. J. McNally, L. O'Reilly, and C. Paulmann, J. X-Ray Sci. Technol. **16**, 215 (2008).
[2] G. Martinez-Criado, B. Alen, A. Homs, A. Somogyi, C. Miskys, J. Susini, J. Pereira-Lachataignerais, and J. Martinez-Pastor, Appl. Phys. Lett. **89**, 221913 (2006).

Downloaded 09 Sep 2011 to 130.199.3.165. Redistribution subject to AIP license or copyright; see http://jap.aip.org/about/rights_and_permissions

[3]L. Soderholm, G. K. Liu, M. R. Antonio, and M. F. Reid, "Characterization of Materials: XEOL/XAFS", K. H. J. Buschow, R. W. Cahn, M. C. Flemings, B. Ilschner, E. J. Kramer, S. Mahajan, and P. Veyssiere, in *Encyclopedia of Materials: Science and Technology* (Elsevier, Oxford, 2001), p. 1140.
[4]S. Emura, T. Moriga, J. Takizawa, M. Nomura, K. R. Bauchspiess, T. Murata, K. Harada, and H. Maeda, Phys. Rev. B **47**, 6918 (1993).
[5]R. A. Rosenberg, G. K. Shenoy, X. H. Sun, and T. K. Sham, Appl. Phys. Lett. **89**, 243102 (2006).
[6]http://absimage.aps.org/image/MWS_MAR10-2009-002928.pdf for R. A. Rosenberg, "*Depth Resolved X-ray Excited Optical Luminescence from SrTiO3*," APS March Meeting Talk, (2010).
[7]K. Hayashi, T. Hayashi, T. Shishido, E. Matsubara, H. Makino, T. Yao, and T. Matsushita, Phys. Rev. B **76**, 014119 (2007).
[8]A. Kazimirov, D. H. Bilderback, R. Huang, A. Sirenko, and A. Ougazzaden, J. Phys. D: Appl. Phys. **37**, L9 (2004).
[9]T. Wunderer, F. Lipski, S. Schwaiger, J. Hertkorn, M. Wiedenmann, M. Feneberg, K. Thonke, and F. Scholz, Jpn. J. Appl. Phys. **48**, 060201 (2009).
[10]T. Wunderer, P. Brückner, J. Hertkorn, F. Scholz, G. J. Beirne, M. Jetter, P. Michler, M. Feneberg, and K. Thonke, Appl. Phys. Lett. **90**, 171123 (2007).
[11]Y. D. Jho, J. S. Yahng, E. Oh, and D. S. Kim, Phys. Rev. B **66**, 035334 (2002).
[12]A. Pinos, S. Marcinkevîĉius, K. Liu, M. S. Shur, J. Yang, M. Shatalov, and R. Gaska, J. Phys. D: Appl. Phys. **41**, 155116 (2008).

Downloaded 09 Sep 2011 to 130.199.3.165. Redistribution subject to AIP license or copyright; see http://jap.aip.org/about/rights_and_permissions